International Journal of Nanoelectronics and Materials
Volume 16, No. 3, July 2023 [523-534]

Synthesis of CdTe nanoparticles by PVD Technique and Study their Physical properties

Ebtehaj F. Jassem[1], Shams B. Ali[1*], and Suad M. Kadhim[1]

[1] Laser and Optoelectronics Engineering Department, University of Technology- Iraq

Received 26 October 2022, Revised 6 December 2022, Accepted 18 December 2022

ABSTRACT

Nano-crystalline CdTe films were coated on a glass substrate by vacuum evaporation (PVD) technique, with the annealed temperature at (25, 100, 150, and 200 °C). The samples were examined by Uv–visible instrument to investigate the transmittance and absorption. The dependency of the absorption coefficient (α) on the wavelength has been investigated. The X-ray diffraction revealed that cubic crystalline was obtained and the peak intensity increased as the temperature increased. The crystallite size increased during grans growth when annealed temperature increased. The estimated energy gaps of the CdTe films were 1.86, 1.87, 1.85, and 1.84 eV, due to the differences in particle sizes. Electrical characteristics have been made to detect the resistivity and conductivity and it was found that the resistivity changes directly with the increase of the energy gap and inversely with the increase in the conductivity of the CdTe films. The surface morphology was homogenous and very smooth surfaces were detected.

Keywords: CdTe films; Optical; structural; electrical properties; surface morphology

1. INTRODUCTION

Cadmium telluride (CdTe) is an essential compound for its uses in energy applications [1] and as a photocathode for water splitting [2]. CdTe films have good electrical characteristics that are favorable for the functioning of solar energy. Cadmium telluride (CdTe) has become the most successful competitor to silicon solar cell material due to its good performance and low-cost solar energy applications. In addition, it is chemically strong and stable, and further nano-layers of this material can be fabricated with various deposition methods over relatively large areas [3]. CdTe has a high absorption of optical radiation and an energy gap of 1.45 eV [4–6]. Improving the efficiency of the solar cell is the most important point for the researchers; the improvement 5 years ago was found by a reform of the CdTe cells with n-layer high transparency. These modifications made the efficiency 21.5% [7] and then enhanced it to 22.1% [8]. It can be synthesized by physical or chemical methods as a thin film. Several deposition methods could be used to prepare CdTe films, including laser ablation [9], electro-deposition, sputtering, spray pyrolysis, and thermal evaporation [10]. Among these techniques, thermal evaporation is a favorable method due to its high deposition rate, low material consumption, and low operating cost. CdTe powder evaporates from heated crucibles at a vacuum of 10^{-5} mbar on glass or any metal substrate.

Multi-layer is prepared by different techniques, categorized into high- or low-temperature procedures, and has a thickness of 2–6 m [11, 12]. CdTe coatings could be polycrystalline or single-crystalline, which can contribute to the modification of their properties [13].

*Corresponding author: Shams.B.Ali@uotechnology.edu.iq

It is notable that the performance of a CdTe solar cell is very powerfully affected and can be dominated by both junctions (emitter or collector) [14].

This article discusses the investigation of the prepared CdTe nanocrystals by thermal evaporation, and studies of optical, morphological, and crystal structural properties were done by several characterization techniques.

2. EXPERIMENT

The fabricated CdTe films were coated on the glass and silicon slides by the PVD method. The substrate was cleaned with Deionized (DI) water and soap for 5 minutes. It was then washed with acetone for 15 minutes, followed by DI water. Then, adapting the voltage to evacuate the chamber with rotary and diffusion pumps about 1.5 hours before the deposition process, the powder was placed on a heated boat made of molybdenum material. The vacuum pressure was 1.5×10^{-4} mbar. The voltage applied on the crucible boat was 80 V, to evaporate CdTe powder into the substrate. The prepared films were annealed at (25, 100, 150, and 200 ^{o}C).

3. RESULTS AND DISCUSSION

3.1 Structural test

The CdTe films were tested by X-ray diffraction as shown in Figure 1. The obtained peaks belong to the cubic (JCPDS files 96-900-8841) space group F-43m. The pattern angles were 23.75, 39.28, 46.44, and 62.41, which correspond to 111, 202, 311, and 313, respectively. By these peaks, crystal structure is confirmed and increased with rising temperature. The plane (111) indicates the strong peak compared with others, This indicates that crystal formation is possible on this plane. The intensity of the peaks increased as the temperature increased [15].

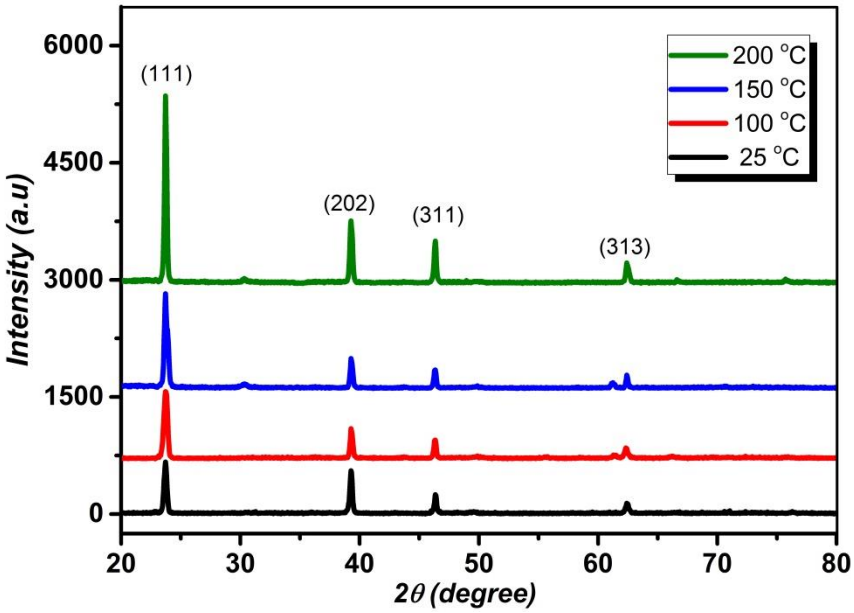

Figure 1. XRD peaks of CdTe thin films

[D = $((0.9\lambda)/(\beta cos\theta))$ [16, 17,18], where is the x-ray wavelength (1.54) and is Bragg's angle, was used to calculate the particle size of CdTe thin films. The lattice constants (a, b, and c)

are important in structural characteristics, and in this work, we obtained cubic structure where ($a = b = c$) and estimated by [19],

$$a = d\sqrt{(h^2 + l^2 + k^2)} \quad (1)$$

where h, k, and l are Miller indices, and (d) the distance was estimated by Eq. (2) [20, 21]];

$$d = \frac{m\lambda}{2sin\theta} \quad (2)$$

where m is one, λ in Å, θ is already known. All achieved data are tabularized in Table 1. Williamson-Smallman's relation was used to calculate dislocation densities (δ). [22, 23]:

$$\delta = \frac{1}{D^2} \quad (3)$$

The specific surface area (SSA) of CdTe coated glass valued by (4):

$$SSA = \frac{6000}{D\rho} \quad (4)$$

where D the crystallite size and (ρ) is the density of CdTe (5.85 g/cm^3).

Due to thermal expansion and a faster rate of growth, higher temperatures have led to larger crystallites, larger crystals, and larger cell volumes as demonstrated in Figure 2(a) similar result confirmed by Mahmood and et.al. [24].

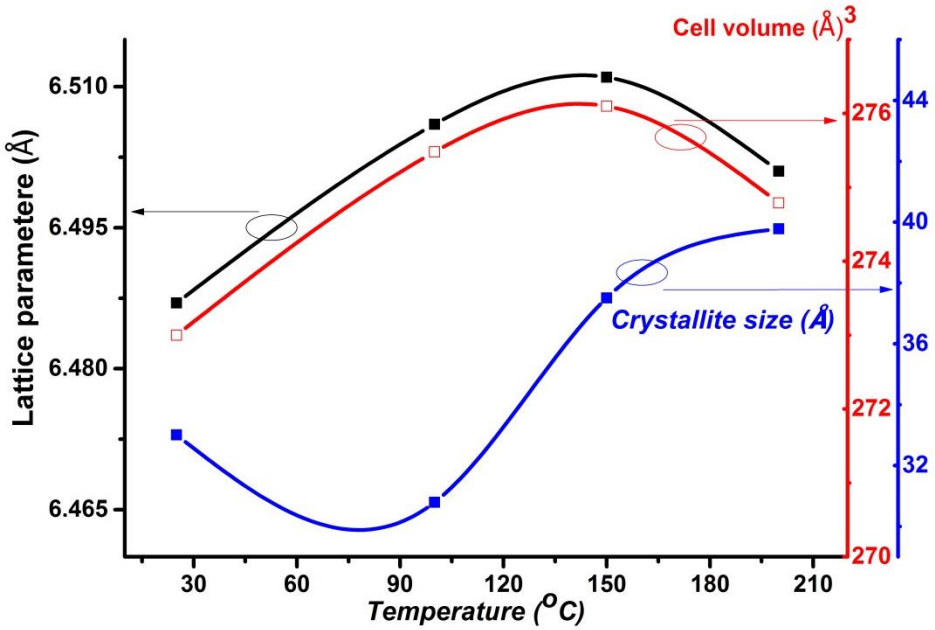

Figure 2. Relation between lattice parameter, cell volume, and crystallite size as a function of annealed temperature

Table 1. Values of *a, b, c*, V, D, δ, *SSA, and packing density*

Specimen Temp. °C	*a=b=c (Å)*	*Cell Volume (Å³)*	*Crystallite size (Å) Scherrer Eq.*	*Dislocation density (Lines/m²) *10¹⁶*	*SSA (m²/g)*	*packing density*	*Angles (α, β, γ) in degree*
25	6.487	273.00	33.01	9.17	310.7	0.911	90

100	6.506	275.48	30.79	10.54	333.1	1.144	90
150	6.511	276.10	37.51	7.10	273.4	1.043	90
200	6.501	274.79	39.78	6.31	257.8	0.872	90

3.2 Electrical test

The current-voltage (I-V) of synthesized CdTe films versus specimen temperature (25–200 °C) were estimated by the Hall Effect test, which showed p-type conductivity for all coated glass. The conductivity (σ_c) was calculated using the formula,

$$\sigma_c = \frac{L}{R \times w \times t_h} \tag{5}$$

where L is the length of the film, R is the thin film resistance, W is the width, and t_h is the film thickness. The resistivity (ρ) was calculated by the conductivity equal,

$$\rho = \frac{1}{\sigma_c} \tag{6}$$

The difference in resistivity, mobility, and conductivity of CdTe films was plotted in Figure 3. It can be noticed that the resistivity increases and then decreases and has an inverse relationship with mobility and conductivity. The films show a low resistivity with increasing temperatures because the electron carriers move more fluidly with increasing crystallite size. [25]. With increasing temperature, conductivity and mobility increase.

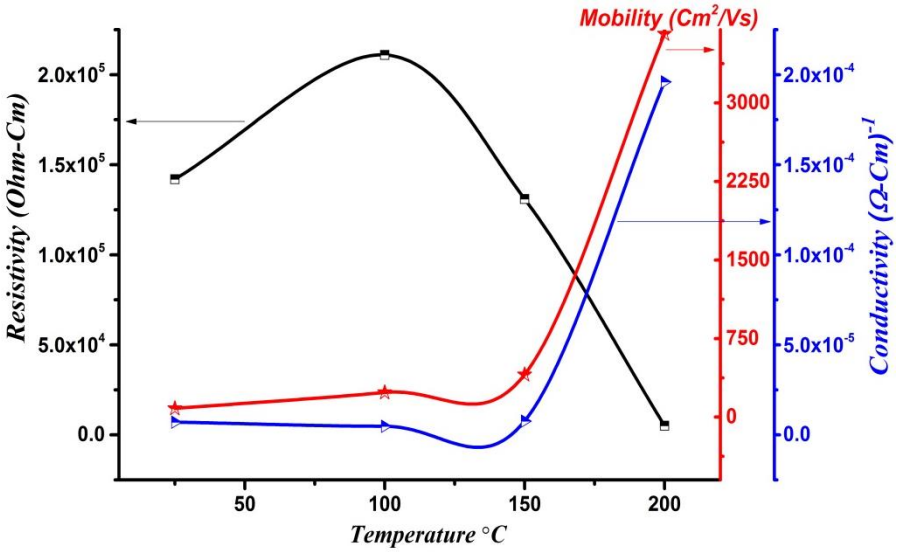

Figure 3. The relation between ρ , $\sigma_c$and mobility as a function of temperature degree

3.3 Optical properties

The transmitted radiations are responsible for electronic transitions by excited sub-shells. The transmittance curves of CdTe thin films were presented in Figure 4. All samples have high transmittance in the near-infrared (> 800 nm). The absorption coefficient, Figure 5, was estimated by the relation, [18, 26, 27],

$$\alpha = 2.303 \frac{A}{t} \tag{7}$$

where (t) is the thickness of the film, (A) is the absorption,

The thicknesses were estimated by the "envelope curve" for T_{max} (T_M), the maximum transmittance and T_{min} (T_m), the minimum transmittance in the transmission, spectra [28]. The refractive index can be expressed as follows:

$$n = \sqrt{N + \sqrt{N^2 - n_s^2}} \tag{8}$$

$$N = 2n_s \frac{T_M - T_m}{T_M T_m} + \frac{n_s^2 + 1}{2} \tag{9}$$

where the refractive index of the substrate (ns) is (in our case, ns = 1.5 for glass).

The equation was used to calculate the thicknesses of the films:

$$t = \frac{\lambda_1 \lambda_2}{2\,(\lambda_1 n_2 - \lambda_2 n_1)} \tag{10}$$

where, n_1 and n_2,the refractive indices corresponding to wavelengths $\boldsymbol{\lambda_1}$ *and* $\boldsymbol{\lambda_2}$, respectively [28].

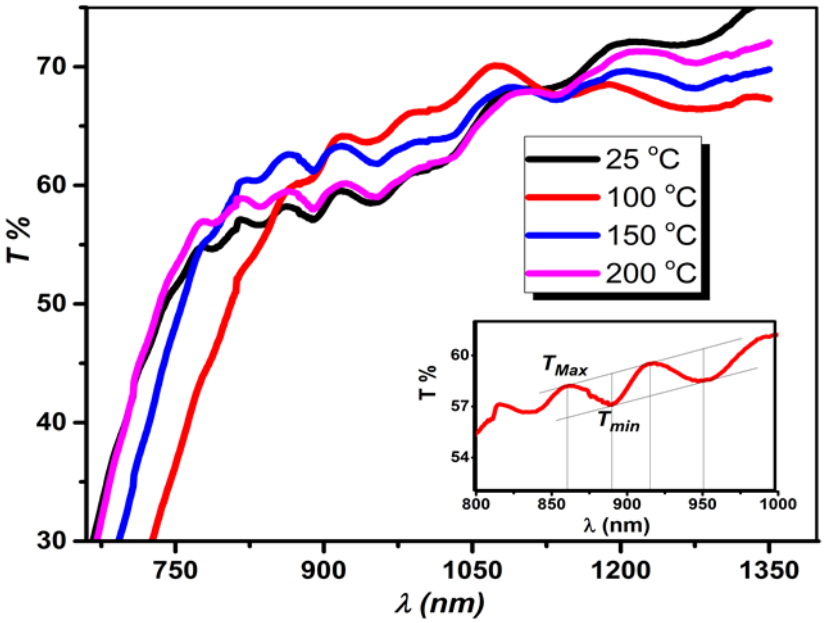

Figure 4. Transmittance curves of CdTe films and transmitted fringes inset

By using the relation between the absorption coefficient and the photon energy (E=hυ), we found the energy gap (E_g), [29],

$$\alpha h\nu = G(h\nu - E_g)^h \tag{11}$$

[30][31]

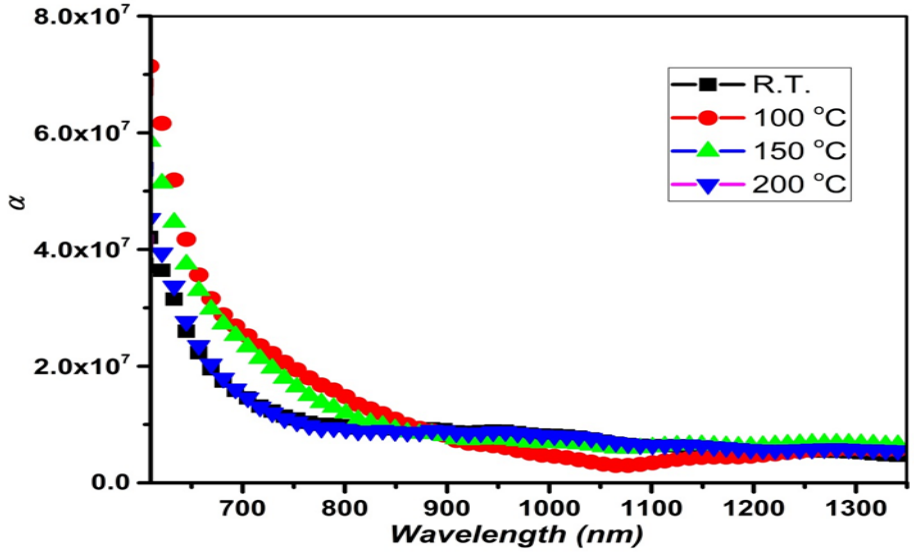

Figure 5. Absorption coefficient plot of CdTe films

Where G is constant, h equals 1/2 or 2 for direct and indirect transitions allowed. These variances in the energy gaps of CdTe originate from the structural differences of the CdTe films during the growth processes. Figure 6 displays Tauc's plots of CdTe thin films. These curves are schemed by $(\alpha h\upsilon)^2$ and $(h\upsilon)$ on the y- and x-axes, respectively. The bandgaps were determined by drawing a line on the x-axis with zero absorption coefficients (α).

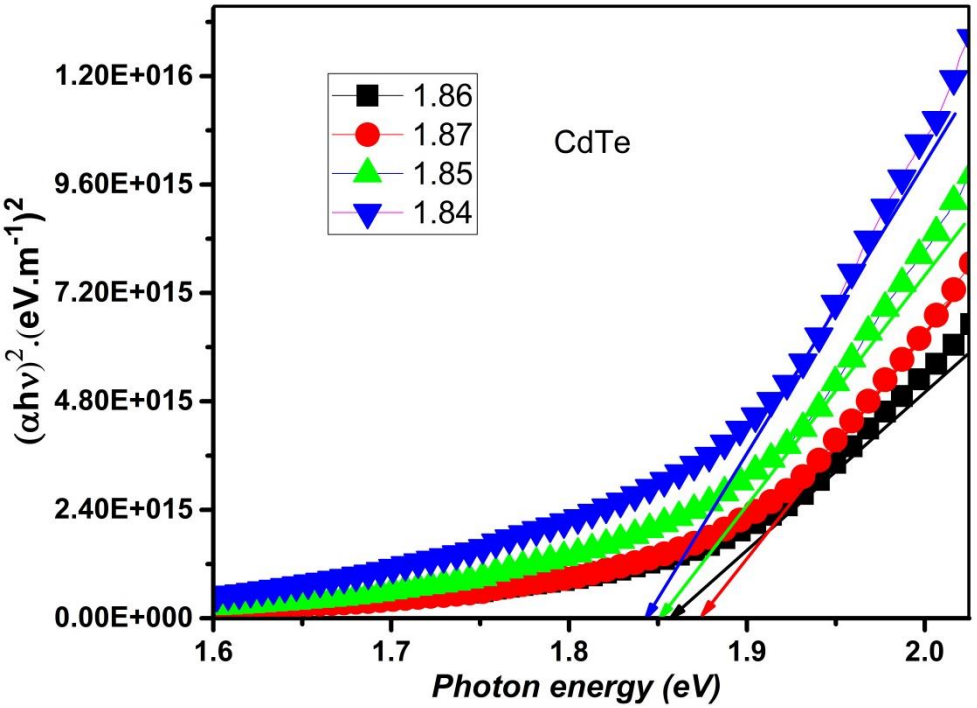

Figure 6. Tauc's plots of CdTe films.

The E_g of CdTe coated glass changed with different temperatures. Eg values obtained were 1.86, 1.87, 1.85, and 1.84 eV The data was tabulating in Table 2. The alteration in the obtained E_g might be due to the size influence of the nanoparticles, and specific surface area, as shown in Figure 7.

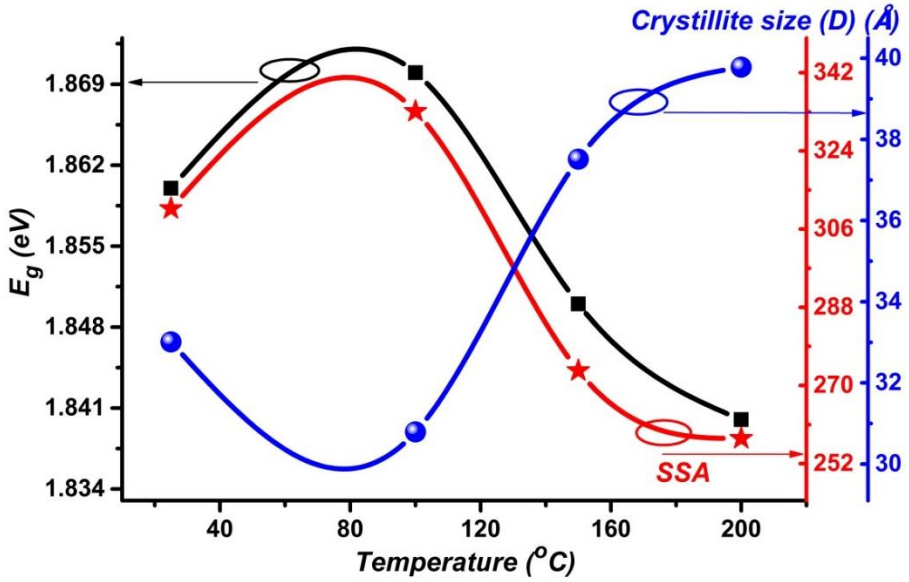

Figure 7. relation of E_g, D, and *SSA*

Table 2. Values of resistivity, mobility, conductivity, and energy gap

Temperature degree (°C)	Resistivity (Ω.Cm)	Mobility Cm^2/Vs	Conductivity $((\Omega.Cm)^{-1}$	Energy gap (nm)
25	1.42E+5	8.24E+1	7.04E-6	1.86
100	2.11E+5	2.35E+2	4.72E-6	1.87
150	1.31E+5	4.05E+2	7.63E-6	1.85
200	5.13E+3	3.66E+3	1.96E-4	1.84

The extinction coefficient (k) was determined using [35]:

$$k = \frac{\alpha\lambda}{4\pi} \tag{12}$$

Another significant characteristic of any film is the refractive index (n), estimated by the relation (13), [32]:

$$n = \frac{1+R}{1-R} + \left[\frac{4R}{(1-R)^2} - k^2\right]^{1/2} \tag{13}$$

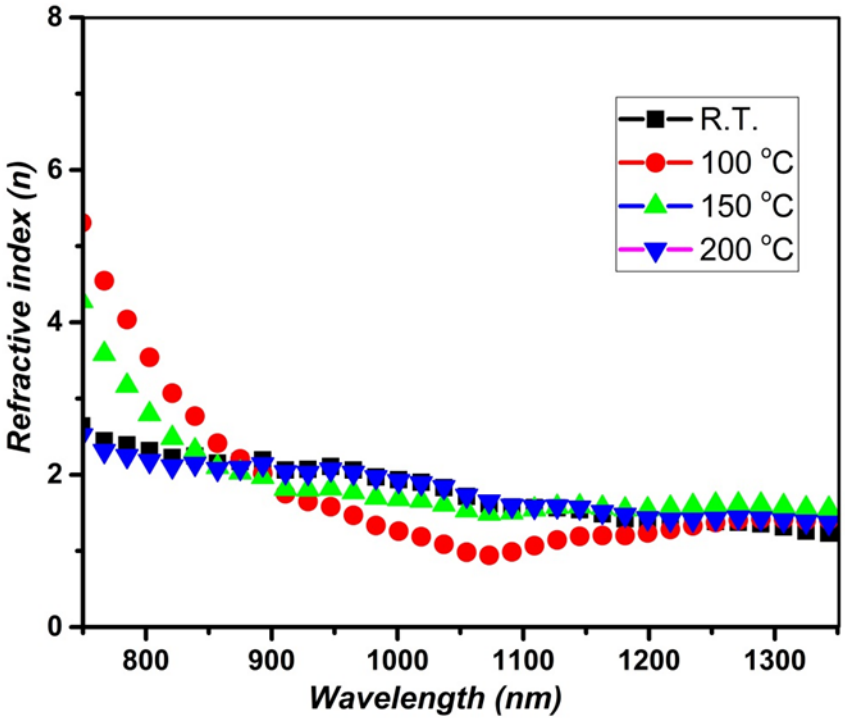

Figure 8. Refractive index plot of CdTe films

The refractive index curves of CdTe films at different temperature treatments drowned with the wavelength, as revealed in Figgure 8. The refractive index (n) was found to be slightly lower within the range (800-1350 nm). It observed that the index of refractive (n) decreased slightly within the range (800–1350 nm). The refractive index is related to the electronic polarization of the materials. The available literature on the refractive index-energy gap [33].

The dielectric constants $\varepsilon_1 and\, \varepsilon_2$ (real and imaginary) are important properties for determining capacitive, resistive, and other defects in the film [34]. See Figure 9, Figure 10 and estimated by,

$$\varepsilon_1 = n^2 - k^2 \quad (14)$$

$$\varepsilon_2 = 2nk \quad (15)$$

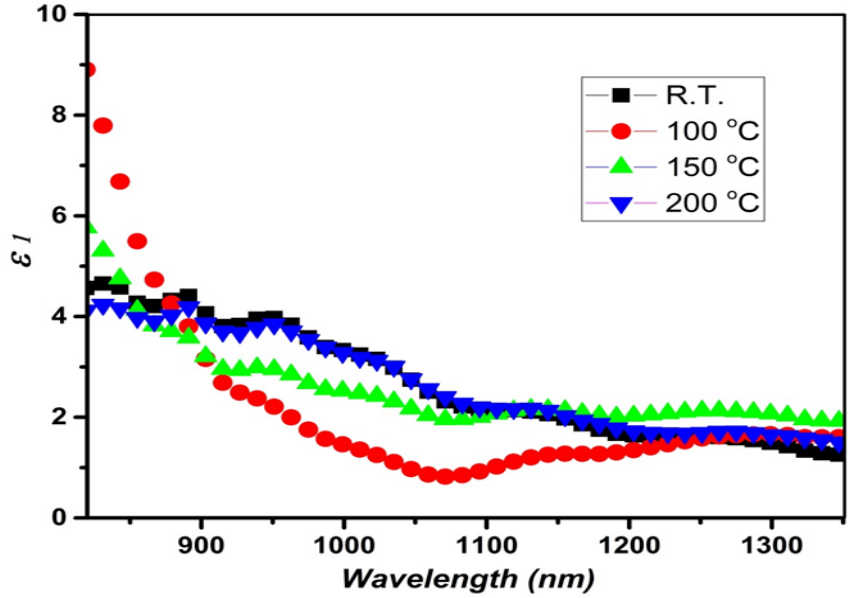

Figure 9. Relation between $\mathcal{E}_1$ and λ

The steady value of the dielectric constant value was discovered to be steady at high values > 1200 nm for all samples.

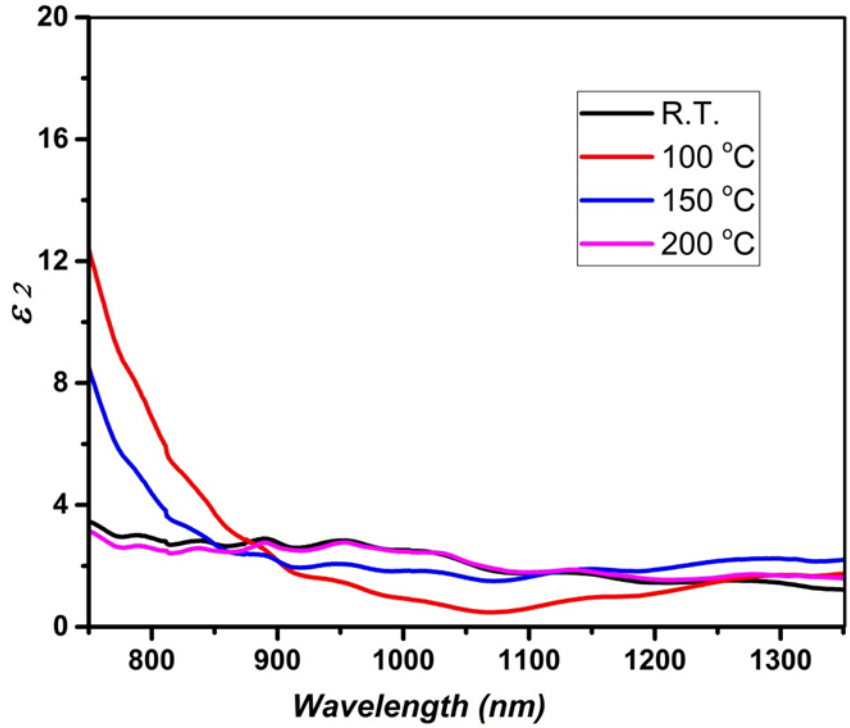

Figure 10. Relation between $\mathcal{E}_2$ and λ

The density (P) is related to the (n) and is valued by the relationship (16) [19]:

$$P = \frac{\rho_f}{\rho_b} = \left(\frac{n_f^2-1}{n_f^2+1}\right)\left(\frac{n_b^2+1}{n_b^2-1}\right) \quad (16)$$

Where nf is the refractive index of coated film and nb is the refractive index of CdTe bulk..

3.5 Topology characteristics

The surface topology images exposed the CdTe films at different temperatures. Figure 12 exhibited a very smooth surface due to the very small nanoparticle size on the surface of the film. It shows a little combined, tiny grain formation. Besides, the deposited surfaces have no cracks with all the films observed. Furthermore, the roughness of the film surfaces increased slightly in some areas, as shown in Figure 12(c, d) versus (a, b).

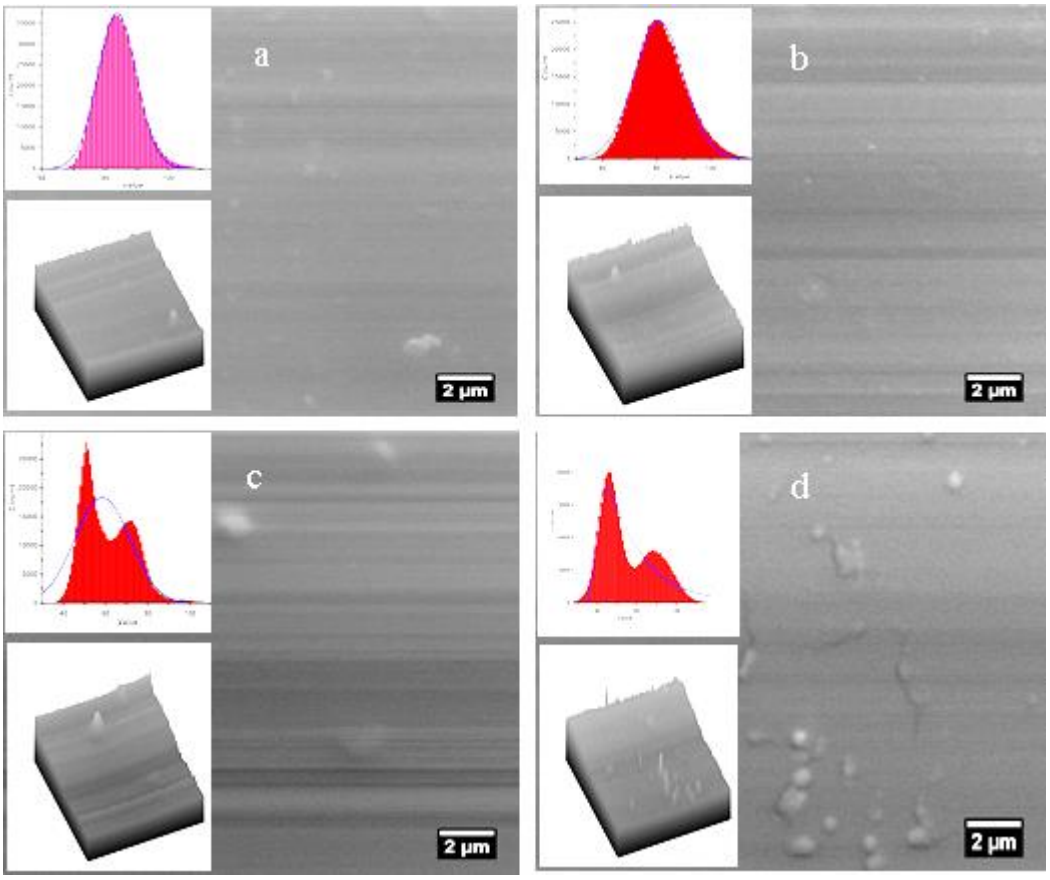

Figure 12. SEM images of CdTe films on glass substrates, (a– room temperature (25 °C, b– 100 °C, c– 150 °C, and d– 200 °C)

4. CONCLUSION

CdTe nanoparticles have been manufactured by the PVD technique. The results presented indicate that the CdTe films have a cubic nanostructure. The XRD peaks displayed the crystallite size increasing as the annealing temperature rose between 150 and 200 °C. Then the cell volume increased. The UV-visible spectra exhibit good transmittance, particularly in the mid-IR range, with fringe due to increased light absorption. The refractive index decreased as the wavelength increased. The band gap variation is coincident with particle size, specific surface area, and conductivity variations, and the relationship among them has been well described. The surface topology presented a very smooth particle. It can be concluded that the synthesized CdTe nanoparticles are suitable for energy applications.

ACKNOWLEDGMENTS

The Uni. of Tech. has supported this work, and the authors appreciate it.

REFERENCES

[1] Hasani, E., Arashti, M. G., Habashi, L. B., & Kamalian, M. Synthesis and deposition of (200)-oriented CdTe thin films on transparent substrates. *Materials Research Express*, *6*(4), 046422, 2019

[2] Su, J.; Minegishi, T.; Katayama, M.; Domen, K. Photoelectrochemical hydrogen evolution from water on a surface modified CdTe thin film electrode under simulated sunlight. J. Mater. Chem. A, 5, 4486–4492, 2017

[3] Romeo, A., & Artegiani, E. CdTe-based thin film solar cells: past, present and future. *Energies*, *14*(6), 1684, 2021

[4] K.-J. Hsiao, Energy-band barrier to improve open-circuit voltage of CdTe solar cells. Sol. Energy Mater. Sol. Cells, 120, 647–653, 2014

[5] M. S. Leite, M. Abashin, H. J. Lezec, A. Gianfrancesco, A. A. Talin, N. B. Zhitenev, Nanoscale Imaging of Photocurrent and Efficiency in CdTe Solar Cells, ACS Nano, 8, 11883–11890, 2014

[6] J. D. Major, R. E. Treharne, L. J. Phillips, K. DuRose, A low-cost non-toxic post-growth activation step for CdTe solar cells, Nature, 511, 334–337, 2014

[7] First Solar Record 21.5 Percent Conversion Efficiency Research Cell Validates Technology Roadmap. 2015, Available online: https://www.sonnenseite.com/en/energy/first-solar-record-21-5-percent-conversion-efficiency-research-cell-validatestechnology- roadmap/ (accessed on 21 January 2021).

[8] Green, M.A.; Dunlop, E.D.; Hohl-Ebinger, J.; Yoshita, M.; Kopidakis, N.; Hao, X. Solar cell efficiency tables (version 56). Prog. Photovolt. Res. Appl. **2020**, 28, 629–638.

[9] Rivera, L. P., García, E., Cardona, D., Pérez-Centeno, A., Camps, E., Santana-Aranda, M. A., ... & Quiñones-Galván, J. G. (2020). CdTe: Sn thin films deposited by the simultaneous laser ablation of CdTe and Sn targets. Materials Research Express, 7(1), 015905.

[10] Ling, Jun, Xulei Zhang, Ting Mao, Lei Li, Shilin Wang, Meng Cao, Jijun Zhang et al. "Electrodeposition of CdTe thin films for solar energy water splitting." Materials 13, no. 7: 1536, 2020

[11] T. D. Lee, A. bong, Thin film solar technologies- a review, 12th nt Conf igh-Capacity pt etworks nabling/Emerging Technol, 33–42, 2015

[12] G. Zeng , J. Zhang, B. Li, L. Wu, W. Li, L. Feng, effect of deposition temperature on the properties of CdTe thin films prepared by close-spaced sublimation, J lectron ater 44(8), 2786–2791, 2015

[13] I. M. Dharmadasa, P. A. Bingham, O. K. Echendu et al., Fabrication of CdS/CdTe-Based Thin Film Solar Cells Using an Electrochemical Technique Coatings, vol. 4, no. 3, pp. 380-415, Jun. 2014, DOI: 10.3390/coatings4030380

[14] Bolkovon Roedern, Photovoltaic Materials, Physics of, 47-59, 2004, ISBN 9780121764807, https://doi.org/10.1016/B0-12-176480-X/00327-2.

[15] M. H. Mohsin, A. A. Salman, Fabrication Solar Cell Device From CdTe Nanoparticles Suspension, Engineering and Technology Journal, 33, 8 Part (B) Scientific, 2015

[16] A. A. Najim, K. R Gbashi, A. T Salih, Synthesis and Characterization of Nanocrystalline Ba-doped Mn_3O_4 Hausmannite Thin Films for Optoelectronic Applications, International Journal of Nanoscience, 20(05), 2150040, 2021

[17] N. B. Mahmood, F. R. Saeed, K. R. Gbashi, U. S. Mahmood, Synthesis and characterization of zinc oxide nanoparticles via oxalate co-precipitation method, Materials Letters: X, 13, 100126, 2022

[18] H. D. Jabar, M. A. Fakhri, M. J. AbdulRazzaq, S. C. Gopinath, The Structural and Optical Investigation of Grown GaN Film on Porous Silicon Substrate Prepared by PLD, Engineering and Technology Journal, 41(2), 1-10, 2023

[19] K. A. Abdulkareem, M. Suad, S. B. Ali, The Structural and Optical Properties of Nanocrystalline Fe3O4 Thin Films Prepared by PLD, Engineering and Technology Journal, 40(02), 334-342, 2022
[20] K. R. Gbashi, S. H. Lafta, N. B. Mahmood, Photo-resistor applications of Bi: ZnSe nano-composition deposited on micro-glass, Optical Materials, 127, 112248, 2022
[21] F. Amer, R. K. Ibrahim, A. N. Naje, S. S. Ahmed, Photoconductive Detector Based on CdTe Nanorods, Engineering and Technology Journal, 33, 6, Part (B) Scientific, 2015
[22] K. R. Gbashi, A. K. Hussein, Cu-doped ZnS coatings for optoelectronics with enhanced protection for UV radiations, Journal of Materials Science: Materials in Electronics, 31(20), 17258-17268, 2020
[23] Pazhanivel T, Nataraj D, Devarajan VP, Mageshwari V, Senthilc K, Soundararajan D (2013) Improved Sensing Performance from methionine capped CdTe and CdTe/ZnS quantum dots for the detection of trace amounts of explosive chemicals in liquid media. Anal Methods 5:910–916. http s://doi.org/10.1039/c2ay26199e
[24] N. B. Mahmood, F. R. Saeed, K. R. Gbashi, A. Hamodi, Z. M. Jaffar, Structural properties of $Co_xCu_{1-x}Fe_2O_4$ solid solution, Journal of the Mechanical Behavior of Materials, *30*(1), 220-227, 2021
[25] M. Thirumoorthi, J. Thomas Joseph Prakash, J. Asian Ceram. Soc. 4, 124–132, 2016
[26] K. R. Gbashi, A. T. Salih, A. A. Najim, M. A. H. Muhi, Nanostructure characteristics of Bi_2O_3: Al_2O_3 thin films and the annealing temperature effect on morphological, optical, and mechanical properties, Superlattices and Microstructures, 146, 106656, 2020
[27] M. A. H. Muhi, K. R. Gbashi, A. T. Salih, A. A. Najim, Novel covellite CuS single-crystal thin films for optoelectronic applications, Plasmonics, 13(1), 247-250, 2018
[28] P. D. File, Joint committee on powder diffraction standards, ASTM, Philadelphia, Pa, 9-185, 1967
[29] A. T. Salih, K. R Gbashi, A. A. Najim, M. A. H. Muhi, Study of structural phase transition in nanocrystalline Cobalt Oxide thin films by pulsed laser deposition, Materials Research Express, 6(7), 076415, 2019
[30] J. H. Khulaef, Effect of Deposition Temperature on Optical and Crystallographic Properties of CsI Thick Films Deposited using Spray Pyrolysis,"Engineering and Technology Journal 35, 2 Part (B) Scientific, 2017
[31] Z. M. Sadiq, M. A. Hassan, K. I. Hassoon, Rod-like Nano-structures of Copper Oxide Prepared by Chemical Bath Deposition, Engineering and Technology Journal, 40(04), 573-581, 2022
[32] K. R. Gbashi, Investigation of morphological, optical and structural properties of multi-layer coatings for solar energy, Applied Physics A, 126(4), 1-7, 2020
[33] Sunil K. Tripathy, Anup Pattanaik, Optical and electronic properties of some semiconductors from energy gaps, Opt. Mater. 53, 123–133, 2016
[34] K. R. Gbashi, M. A. H. Muhi, A. A. Jabbar, N. B. Mahmood, R. F. Hasan, Copper dopants impact enhanced behavior of Mn: Cu co-doped CdS nanocrystals (quantum dots) and their characteristics for optoelectronic applications, Applied Physics A, 126(8), 1-16, 2020